



# RNA-binding protein RBM28 can translocate from the nucleolus to the nucleoplasm to inhibit the transcriptional activity of p53

Received for publication, August 21, 2021, and in revised form, December 10, 2021. Published, Papers in Press, December 22, 2021,

<https://doi.org/10.1016/j.jbc.2021.101524>

Xin Lin<sup>1,‡</sup>, Liwen Zhou<sup>1,‡</sup>, Jianliang Zhong<sup>1</sup>, Li Zhong<sup>1,2</sup>, Ruhua Zhang<sup>1</sup>, Tiebang Kang<sup>1,\*</sup>, and Yuanzhong Wu<sup>1,\*</sup>

From the <sup>1</sup>State Key Laboratory of Oncology in South China, Sun Yat-sen University Cancer Center, Collaborative Innovation Center for Cancer Medicine, Guangzhou, China; <sup>2</sup>Scientific Research Center, The Seventh Affiliated Hospital, Sun Yat-sen University, Shenzhen, China

Edited by Phyllis Hanson

RNA-binding protein RBM28 (RBM28), as a nucleolar component of spliceosomal small nuclear ribonucleoproteins, is involved in the nucleolar stress response. Whether and how RBM28 regulates tumor progression remains unclear. Here, we report that RBM28 is frequently overexpressed in various types of cancer and that its upregulation is associated with a poor prognosis. Functional and mechanistic assays revealed that RBM28 promotes the survival and growth of cancer cells by interacting with the DNA-binding domain of tumor suppressor p53 to inhibit p53 transcriptional activity. Upon treatment with chemotherapeutic drugs (e.g., adriamycin), RBM28 is translocated from the nucleolus to the nucleoplasm, which is likely mediated *via* phosphorylation of RBM28 at Ser122 by DNA checkpoint kinases 1 and 2 (Chk1/2), indicating that RBM28 may act as a nucleolar stress sensor in response to DNA damage stress. Our findings not only reveal RBM28 as a potential biomarker and therapeutic target for cancers but also provide mechanistic insights into how cancer cells convert stress signals into a cellular response linking the nucleolus to regulation of the tumor suppressor p53.

The nucleolus is associated with the regulation of several major physiological cellular processes including ribosome assembly, cell mitosis, stress responses, and ribonucleoprotein complex generation (1). Recent landmark proteomic studies have led to the discovery of more than 4500 nucleolus-associated proteins, and 70% of nucleolar proteins have functions unrelated to the production of ribosome subunits, including the regulation of cell cycle progression, DNA damage sensing and repair, genomic organization, nuclear architecture establishment, and global gene expression, suggesting that nucleolar functions might be significantly broader than previously thought (2). Recently, the nucleolus has gained attention for its novel role in the regulation of cellular stress (3). Nucleolar stress is emerging as a new concept and is characterized by various stressor-induced impairments in

nucleolar morphology and function that ultimately lead to disturbances in cell homeostasis through the activation of p53 or other stress signaling pathways (4). The following elements are described as hallmarks of nucleolar stress: a wide range of stimuli as stressors cause disturbances in ribosome biogenesis, nucleoplasmic translocation of nucleolar proteins, morphological alterations in nucleolar stress, impaired rRNA transcription and processing, and activation of p53 signaling and involvement of p53-independent stress signaling (4). Theoretically, nucleoli do not possess defined structural barriers and thus may not have a system akin to nuclear transport machinery (such as importins, a nuclear pore complex, and exportins); proteins that localize to nucleoli can potentially traffic in and out of the nucleolus in a relatively free manner (5). Present studies have shown that the translocation of nucleolar proteins in nucleolar stress signaling mainly relies on specific interactions with binding sites within nucleolar components, which raises the question of the identity of the molecular mechanism involved in protein nucleolar targeting. Posttranslational modifications (PTMs) of nucleolar proteins are also speculated to play a major role in stress-induced changes in protein localization. For instance, during nucleolar oxidation, NPM1 undergoes S-glutathionylation on cysteine 275, which triggers the dissociation of NPM1 from nucleolar nucleic acids, resulting in the nucleoplasmic translocation and activation of p53 (6).

RNA-binding protein (RBP) is a general term for a class of proteins that bind to RNA. RBPs are highly conserved across species and play key roles in maintaining gene expression homeostasis. Mounting evidence has shown that RBPs are involved in various important cellular processes, such as cell transport, localization, differentiation, and metabolism by regulating RNA splicing, polyadenylation, mRNA stability, mRNA localization, and translation through interactions with coding and noncoding RNAs and other proteins (7). A recent global survey of proteins that are UV cross-linkable to RNA revealed a large number of both canonical and noncanonical RBPs (8). Recent studies also found that RBPs have some nontraditional functions, such as participating in gene transcription regulation and acting as sensors for cellular stress signals through p53 activation (3, 8). Several studies have

<sup>‡</sup> These authors contributed equally to this work.

\* For correspondence: Yuanzhong Wu, [wuyzh@sysucc.org.cn](mailto:wuyzh@sysucc.org.cn); Tiebang Kang, [kangtb@sysucc.org.cn](mailto:kangtb@sysucc.org.cn).

## RBM28 inhibits p53 via nucleolus–nucleoplasm translocation

provided evidence to link known cancer drivers to abnormal expression or altered activity of RBPs; however, the extent to which RBPs act on cancer progression remains unclear, and further exploration of RBP functions and their regulatory networks may provide new molecular targets for cancer therapy.

RBPs are well documented to be subjected to a variety of PTMs including acetylation, phosphorylation, methylation, and ubiquitination (9). PTMs alter RBP binding properties, functions, or subcellular localization. Notably, the PTMs of RNA-binding elements in RBPs are particularly prominent (7). Abnormal modification of these sites may be one of the main factors leading to RBP dysfunction in tumors (7), and many studies have shown that abnormal expression or mutation in the RNA-binding motif family plays a very important role in the occurrence and metastasis of tumors (10). For example, RBM10 activates key proliferative signaling pathways, including the epidermal growth factor receptor, mitogen-activated protein kinase, and phosphatidylinositol-3-kinase (PI3K)-Akt pathway and inhibits apoptotic pathways in lung adenocarcinoma (11). RBM14 promotes radioresistance in glioblastoma by regulating DNA damage repair and cell differentiation (12). RBM28, as a nucleolar component of spliceosomal small nuclear ribonucleoproteins (snRNPs) may also play roles in cancer progression by involving in the nucleolar stress response. According to bioinformatics analysis, head and neck squamous cell carcinoma and lung squamous cell carcinoma share common splicing alterations, nearly half of which are associated with RBM28 (13). The binding motifs of RBM28 were significantly enriched in the 3'UTR of nonsmall cell lung cancer patient's platelet RNAs (14). However, whether and how RBM28 regulates tumor progression remain unclear. In this report, we found that Chk1 and Chk2 phosphorylate RBM28 at S122 upon DNA damage, promoting RBM28 nucleolar–nucleoplasmic translocation, where RBM28 directly binds to p53 to suppress the transcriptional activity of p53.

## Results

### RBM28 may act as an oncogene in various cancers

To explore the potential cancer driver genes in the RNA-binding motif family, we analyzed gene dependency scores in 903 cancer cell lines from the DepMap database and found that *RBM28* is one of the highest cancer-dependent genes (Fig. 1A). Interestingly, as shown in the Clinical Proteomic Tumor Analysis Consortium proteome database, RBM28 protein levels were upregulated in a variety of cancers, such as colon cancer, clear cell renal cell carcinoma, uterine corpus endometrial carcinoma, ovarian cancer, breast cancer, and lung adenocarcinoma (Fig. 1B). According to The Cancer Genome Atlas transcriptome data and patient survival information, a high mRNA level of *RBM28* was associated with a poor prognosis in multiple cancer types, including breast cancer, uterine corpus endometrial carcinoma, clear cell renal cell carcinoma, lung adenocarcinoma, hepatocellular carcinoma, and all types of sarcomas (Fig. 1C). These results suggest that RBM28 may act as an oncogene in various cancers.

### RBM28 plays a crucial role in the growth of cancer cells

To investigate the role of RBM28 in cancer progression, we constructed constitutive HCT116 and U2OS cell lines with RBM28 KO using CRISPR-Cas9 technology. The knockout efficiency was determined by Western blot (Fig. 2A). According to 3-(4, 5-dimethylthiazol-2-yl)-2, 5-diphenyltetrazolium bromide assay and colony formation assay, RBM28 KO significantly reduced the proliferation of both HCT116 and U2OS cells (Fig. 2, B and C). More importantly, RBM28 KO significantly reduced the growth of subcutaneous tumors, as determined using xenografts of HCT116 cells in mice (Fig. 2, D and F), which was supported by the finding that RBM28 KO decreased the cell proliferation index, determined by Ki-67 immunohistochemistry staining using these xenografts (Fig. 2G). These results indicated that RBM28 plays a crucial role in the growth of cancer cells.

### RBM28 impairs the transcriptional activity of p53 by reducing the binding of p53 to its target gene promoters

Next, we explored how RBM28 promotes cell proliferation. We conducted an RNA-seq in RBM28 KO U2OS cells, which identified 1525 different expression genes, with 1003 upregulated and 522 downregulated. Kyoto Encyclopedia of Genes and Genomes pathway enrichment analysis demonstrated that p53-related pathways were significantly enriched in RBM28 KO cells *versus* control cells (Fig. 3A). A representative heatmap from global comparative transcriptome analysis indicated that p53 target genes were upregulated upon RBM28 KO (Fig. 3B). These results were validated by our qPCR results, showing that RBM28 depletion and ectopic RBM28 increased and decreased the expression of *CDKN1A*, *FAS*, *GADD45A*, and *SERPINE1*, respectively (Fig. 3, C and D).

We further confirmed the effect of RBM28 on p53 using *CDKN1A* as the representative. According to dual luciferase reporter assay and chromatin immunoprecipitation (ChIP) assay, RBM28 depletion increased *CDKN1A* promoter activity and the binding of p53 to the *CDKN1A* promoter in U2OS cells (Fig. 3, E and F). More importantly, p21, which is the protein product encoded by *CDKN1A* was upregulated in p53 WT cells but not p53 null cells, suggesting that the effect of RBM28 on p53 target genes was p53-dependent (Fig. 3G). Collectively, these results suggested that RBM28 may impair the transcriptional activity of p53 by reducing the binding of p53 to its target gene promoters. In addition, reduction in the colony formation by depletion of RBM28 was weaker in HCT116 p53<sup>-/-</sup> cells than that in HCT116 p53<sup>+/+</sup> cells, as shown in Fig. S1, indicating that RBM28 has other downstream effectors besides p53. This is consistent with the DepMap data results that RBM28 is required for cancer proliferation both in p53 WT and mutant cell lines, as shown in Fig. S2. Together, these results indicated that p53 is one of the downstream effectors of RBM28 to maintain cell proliferation.

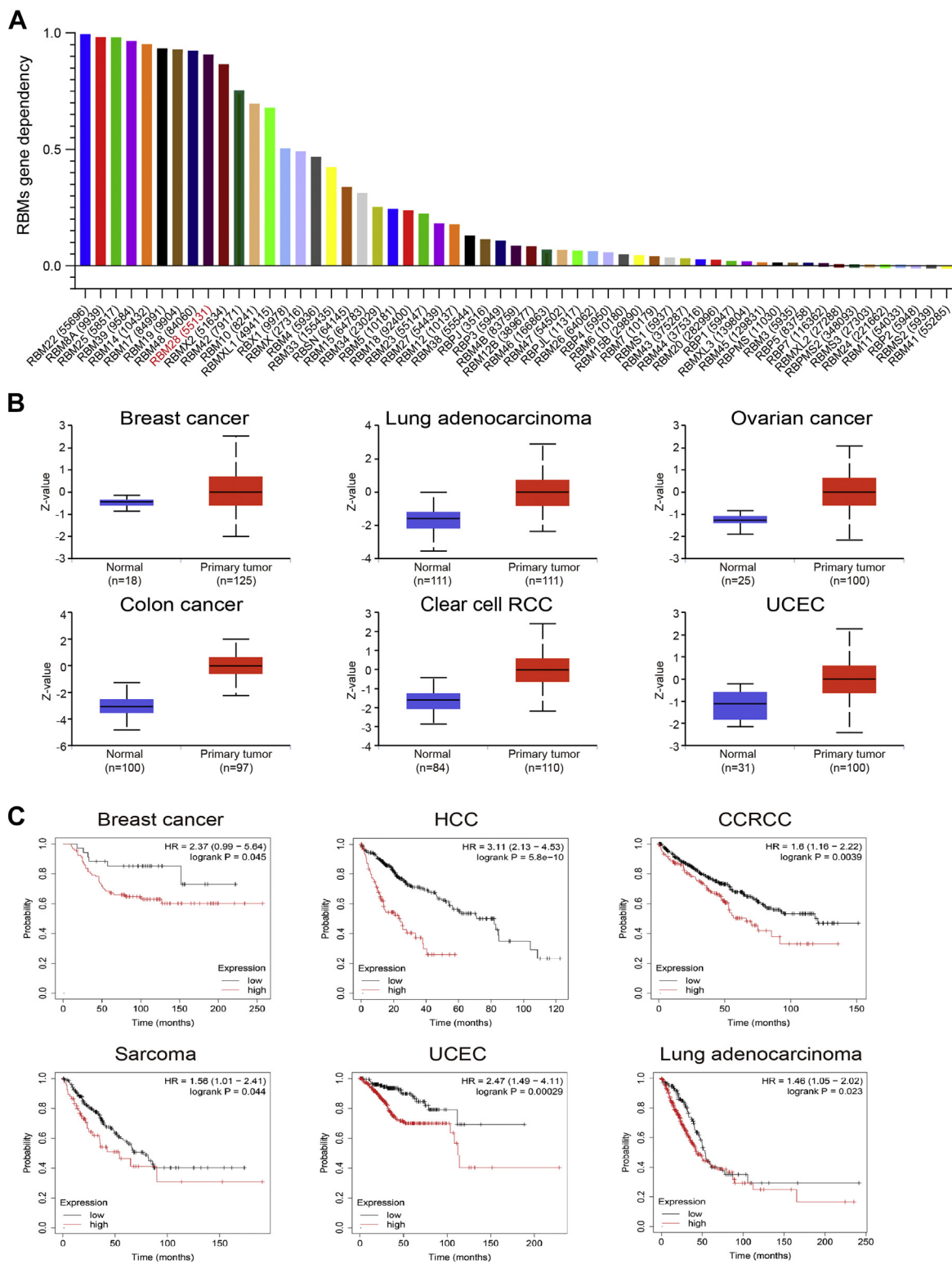


**Figure 1. RBM28 was elevated in various cancer types and associated with a poor patient prognosis.** A, the RBM dependency scores from 903 cancer cell lines representing nearly all types of cancers were analyzed based on DepMap. The probabilities of dependency are the average of each gene score in a cell line. The numbers close to 1.0 is considered more dependent. B, the protein levels of RBM28 in colon cancer, clear cell renal cell carcinoma, ovarian cancer, uterine corpus endometrial carcinoma, and breast cancer were based on the CPTAC database. Unpaired Student's *t* test. C, TCGA survival analysis for breast cancer, liver hepatocellular carcinoma, kidney renal clear cell carcinoma, all types of sarcomas, uterine corpus endometrial carcinoma, and lung adenocarcinoma cancer patients based on RBM28 expression. The log-rank test was used for statistical analysis. *p* values are shown. CCRCC; clear cell renal cell carcinoma; CPTAC; Clinical Proteomic Tumor Analysis Consortium; HCC; hepatocellular carcinoma; RCC; renal cell carcinoma; TCGA; The Cancer Genome Atlas; UCEC; uterine corpus endometrial carcinoma.

## RBM28 inhibits p53 via nucleolus–nucleoplasm translocation

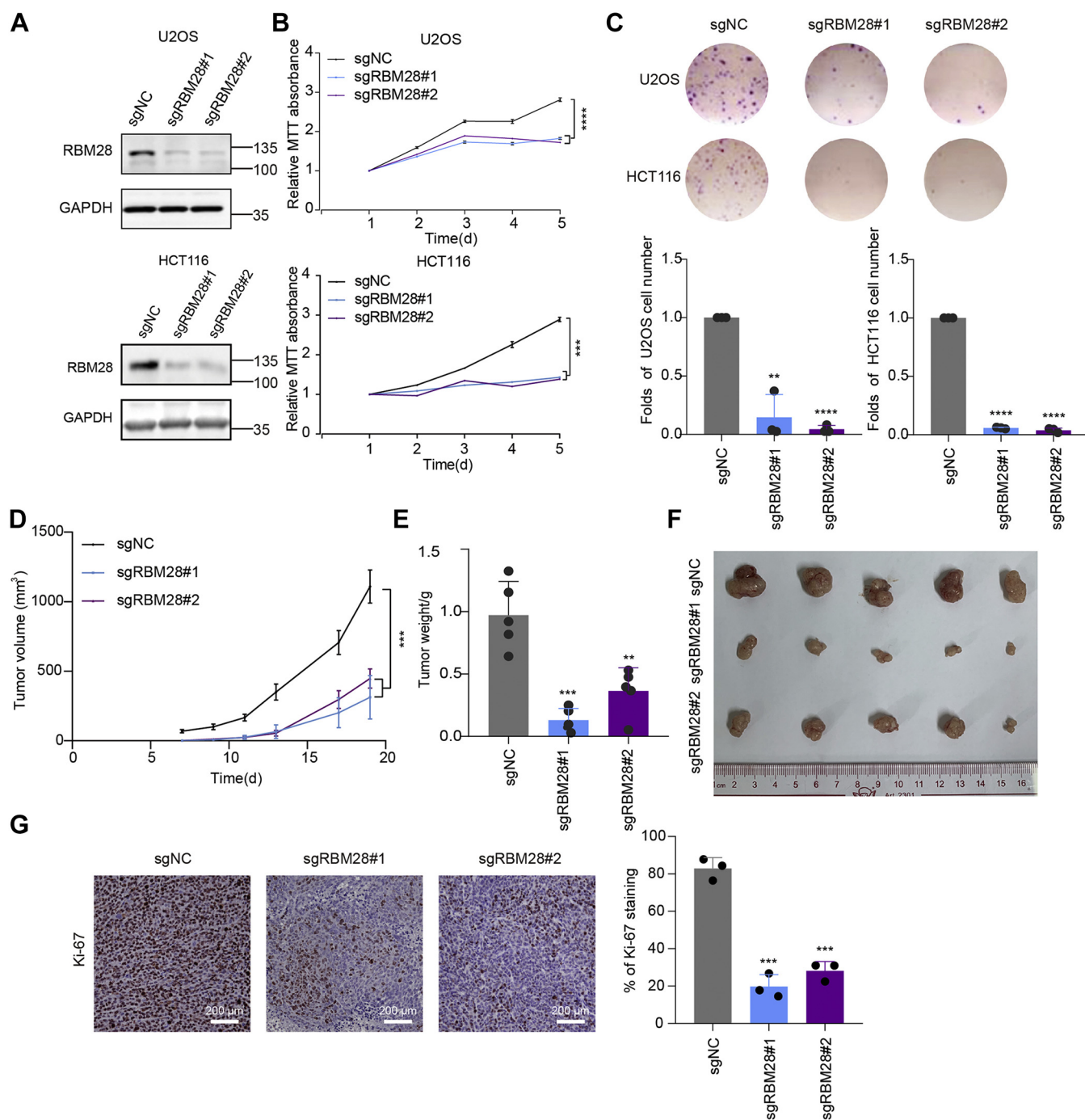


**Figure 2. RBM28 promotes cancer cell proliferation and growth.** A–C, the indicated stable U2OS cells or HCT116 cells were subjected to Western blot (A), MTT assay (B), and colony formation assay (C). The data are the mean  $\pm$  SD,  $n = 8$ , \*\*\*\* $p < 0.0001$  by two-way ANOVA for (B) and  $n = 3$ , \*\* $p < 0.01$ , \*\*\*\* $p < 0.0001$  by unpaired Student's  $t$  test for (C). D–F, the indicated stable HCT116 cells were inoculated subcutaneously into nude mice. Tumor volumes were measured twice a week (D), and tumor weights (E) and tumor images (F) were recorded. The data are the mean  $\pm$  SD,  $n = 5$ . \*\*\* $p < 0.001$  by two-way ANOVA for (D) and \*\*\* $p < 0.001$ , \*\*\*\* $p < 0.0001$  by unpaired Student's  $t$  test for (E). G, representative immunohistochemical staining of Ki-67 from xenograft tumors using the indicated stable HCT116 cells. The scale bar represents 200  $\mu$ m. The data are the mean  $\pm$  SD,  $n = 3$ . \*\*\* $p < 0.001$  by unpaired Student's  $t$  test. MTT, 3-(4, 5-dimethylthiazol-2-yl)-2, 5-diphenyltetrazolium bromide.

### RBM28 interacts with the DNA binding domain of p53 through multiple regions

Upon DNA damage, acetylation at Lys382 and phosphorylation at Ser15 are critical events in p53 activation (15, 16). However, depletion of RBM28 did not affect p53 acetylation at Lys382, phosphorylation at Ser15, or the total p53 level with or

without adriamycin (ADR) treatment (Fig. S3). RBM28 KO did not affect the half-life of *CDKN1A* mRNA (Fig. S4). Given that RBM28 may impair the transcriptional activity of p53 by reducing the binding of p53 to its target gene promoters, as shown above (Fig. 3, E and F), we surmised that RBM28 may bind to p53. Indeed, RBM28 interacts with p53 at their

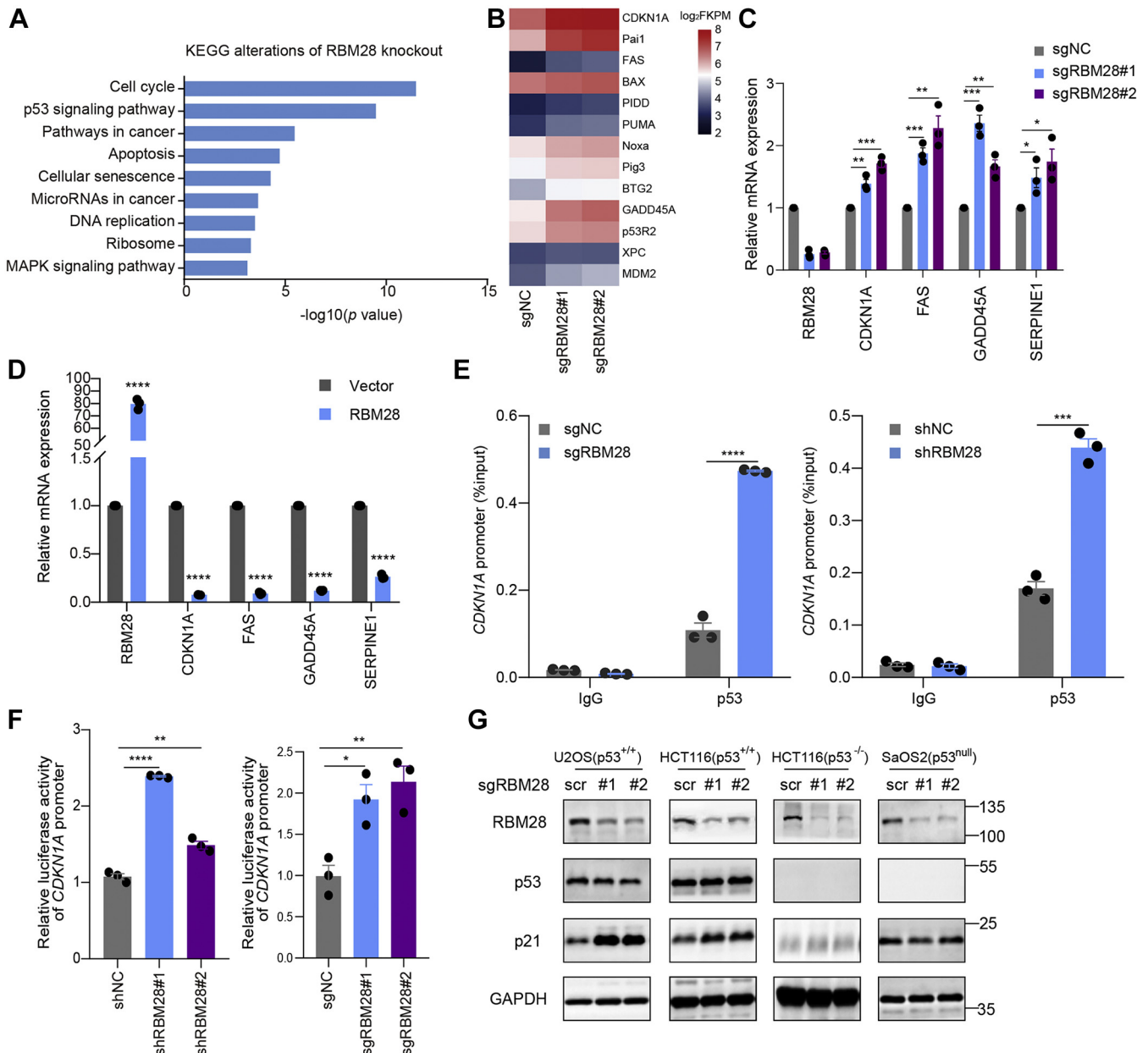


**Figure 3. RBM28 inhibits the transcription activity of p53.** *A*, KEGG pathway enrichment analysis of U2OS cells with RBM28 depletion. *B*, representative heatmap from the global comparative transcriptome analysis indicating the genes that were upregulated upon RBM28 knockout. *C* and *D*, qRT-PCR was used to detect the relative mRNA expression levels of *CDKN1A*, *FAS*, *GADD45A*, or *SERPINE1* in the indicated stable U2OS cells. The data are the mean  $\pm$  SD,  $n = 3$ . \* $p < 0.05$ , \*\* $p < 0.01$ , \*\*\* $p < 0.001$ , \*\*\*\* $p < 0.0001$  by unpaired Student's *t* test. *E*, a luciferase reporter assay was used to detect the promoter activity of *CDKN1A* upon RBM28 knockout or knockdown. The data are the mean  $\pm$  SD,  $n = 3$ . \*\* $p < 0.01$  by unpaired Student's *t* test. *F*, a ChIP-qPCR assay was performed to detect the binding ability of p53 to the *CDKN1A* promoter in the indicated stable U2OS cells. The data are the mean  $\pm$  SD,  $n = 3$ . \*\*\* $p < 0.001$ , \*\*\*\* $p < 0.0001$  by unpaired Student's *t* test. *G*, the indicated cell lines under the indicated treatments were subjected to Western blot. ChIP, chromatin immunoprecipitation; KEGG, Kyoto Encyclopedia of Genes and Genomes.

endogenous levels (Fig. 4A), and this interaction using exogenous RBM28 and p53 was not affected by the RNase A treatment, indicating that the interaction of RBM28 with p53 is RNA-independent (Fig. 4B).

Next, we attempted to determine the regions responsible for the interaction between RBM28 and p53. A series of fragments of p53 and RBM28 were generated, and coimmunoprecipitation was performed (Fig. S5, A and B). The DNA-binding domain of p53 (residues 100–300) was

necessary and sufficient to bind to RBM28 (Fig. 4C). Interestingly, three separate regions of RBM28, residues 1 to 95, 96 to 258, and 468 to 759, could interact with p53 (Fig. 4D). We further generated several mutants of RBM28 by depleting different regions (Fig. S5C). The interaction between RBM28 and p53 was not diminished by truncation of any particular region (Fig. 4E). These results revealed that RBM28 may interact with the DNA-binding domain of p53 through multiple regions.

## RBM28 inhibits p53 via nucleolus–nucleoplasm translocation

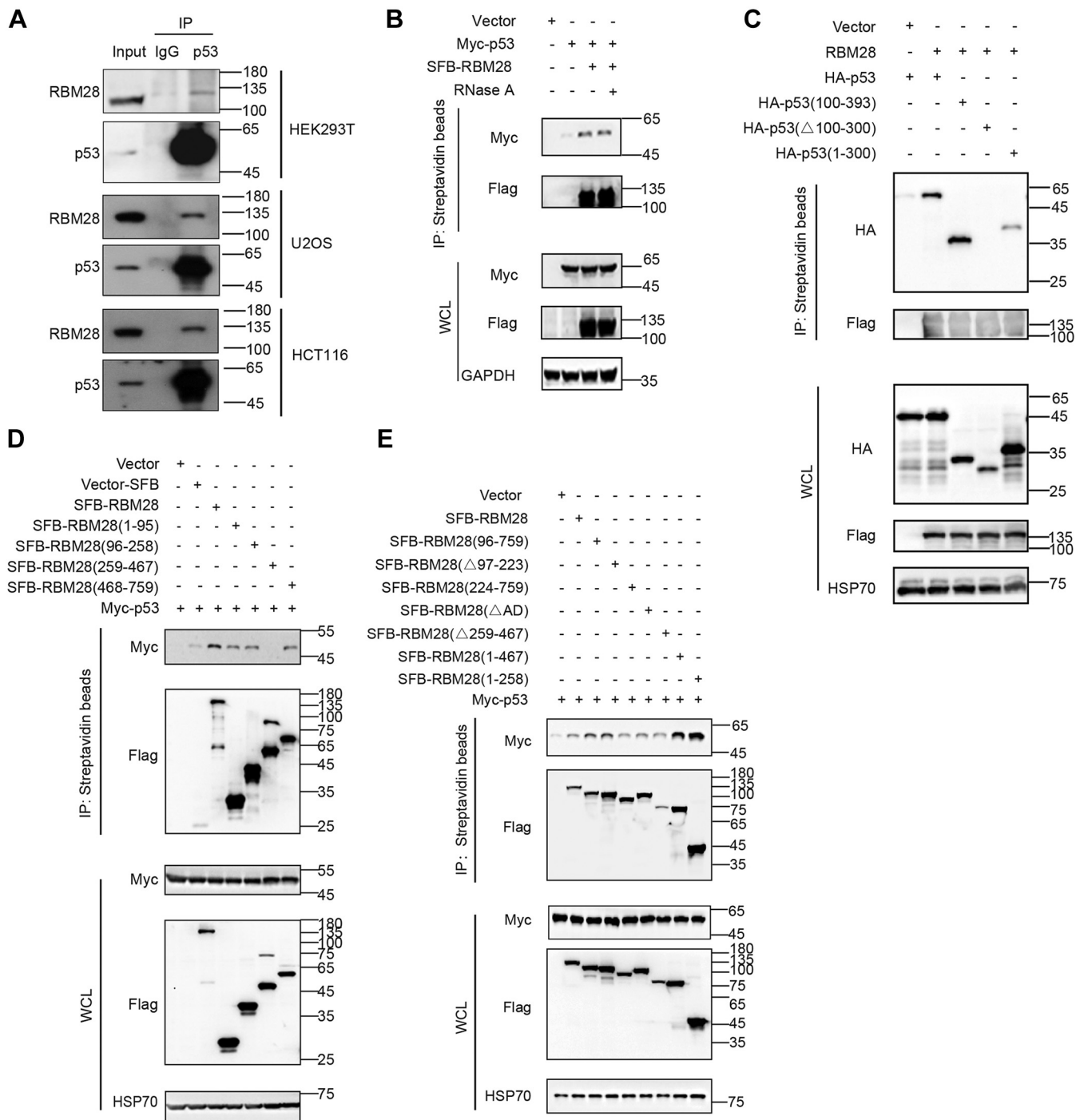


**Figure 4. RBM28 binds to the DNA binding domain of p53 through multiple regions.** A, HEK293T, U2OS, and HCT116 cells were lysed with RIPA, and the lysates were subjected to immunoprecipitation using IgG or anti-p53 antibody, and were analyzed by Western blot. B, HEK293T cells were transfected with the indicated plasmids for 48 h. Then, the cells were lysed and treated with or without RNase A (5 ng/ $\mu$ l) and analyzed by Western blot or immunoprecipitated with streptavidin beads followed by Western blot. C, HEK293T cells cotransfected with SFB-RBM28 and various p53 mutants as indicated for 48 h. Then, the cells were lysed and analyzed by Western blot or immunoprecipitated with streptavidin beads followed by Western blot. D and E, HEK293T cells cotransfected with Myc-p53 and various RBM28 mutants as indicated for 48 h. Then, the cells were lysed and analyzed by Western blot or immunoprecipitated with streptavidin beads followed by Western blot. HEK, human embryonic kidney.

### Chk1/Chk2 promotes the nucleolar–nucleoplasmic translocation of RBM28 induced by ADR

The nucleolus is considered a major hub in coordination of the stress response (17). Nucleolar stress causes many nucleolar molecules to redistribute in the nucleus, that is, to be released from the nucleolus to the nucleoplasm (4). Given that

RBM28 is a nucleolar protein (Fig. S6) whereas p53 serves as a transcription factor in the nucleoplasm, we speculated whether RBM28 might undergo nucleolar–nucleoplasmic translocation upon cellular stress. After applying a series of stressors, as shown in Figure 5A, we found that nucleoplasmic localization of RBM28 significantly increased upon treatment with

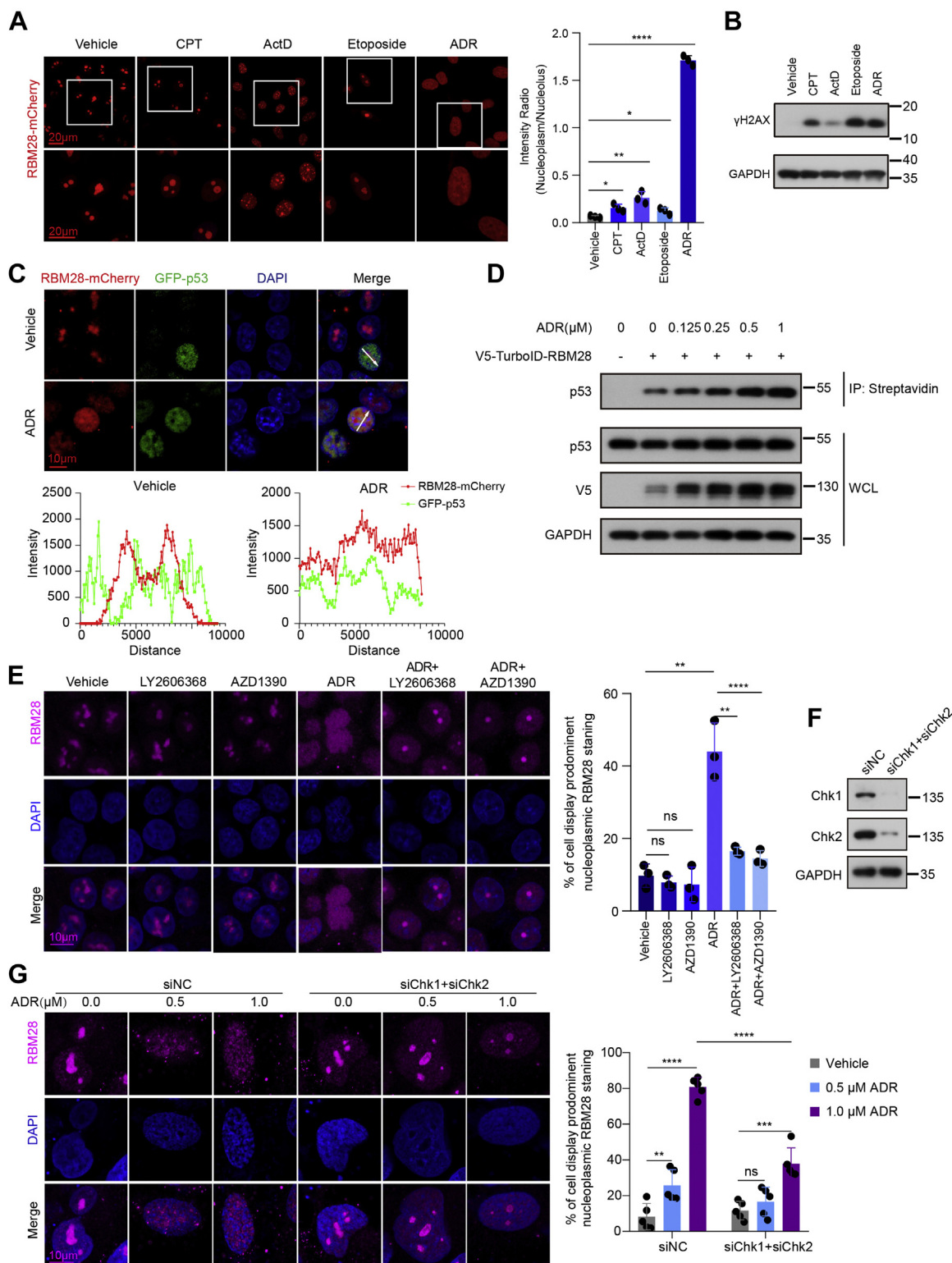


**Figure 5. Chk1/Chk2 promote nucleoplasmic localization of RBM28 upon treatment with chemodrugs.** *A*, RBM28-mCherry (red)-transfected A375 cells were treated with ADR (1 µM), CPT (4 µM), ActD (5 µg/ml), or etoposide (20 µM) for 12 h and visualized by fluorescence microscopy, followed by calculation of the intensity ratio of the nucleoplasm to nucleolus. The scale bar represents 20 µm. The data are the mean ± SD,  $n = 3$ . \* $p < 0.05$ , \*\* $p < 0.01$ , \*\*\*\* $p < 0.0001$  by unpaired Student's *t* test. *B*, Western blot was used to detect the expression of γH2AX. *C*, RBM28-mCherry (red) and GFP-p53 (green) were cotransfected into HCT116 cells in the presence or absence of ADR (1 µM, 6 h), and nuclei were stained with DAPI (blue). The scale bar represents 10 µm. *D*, HEK293T cells were transfected with indicated plasmids for 24 h, followed by treatment with indicated concentrations of ADR for another 24 h. Before harvesting, the cells were treated with 50 µM biotin for 30 min, followed by RIPA-SDS lysis, sonication, and Streptavidin IP. *E*, immunofluorescence assays were performed to observe the subcellular localization of endogenous RBM28 (violet) and nuclei (blue) in HCT116 cells treated with LY2606368 (30 nM, 12 h) and AZD1390 (30 nM, 12 h) in the presence or absence of ADR (1 µM, 6 h). The data are the mean ± SD,  $n = 3$ ; ns, no significance, \*\* $p < 0.01$  by unpaired Student's *t* test. *F*, the Chk1 and Chk2 were knocked down by specific siRNAs in HCT116 cells. Western blot was used to validate the knockdown efficiency. *G*, immunofluorescence assays were performed to observe the subcellular localization of endogenous RBM28 (violet) and DAPI (blue) in HCT116 cells

## RBM28 inhibits p53 via nucleolus–nucleoplasm translocation

DNA-damaging agents commonly used in cancer chemotherapy, such as ADR, camptothecin, actinomycin D (ActD), and etoposide (18, 19). The DNA damage induced by each agent was determined by the detection of  $\gamma$ H2AX expression (Fig. 5B). In response to the ADR treatment, ectopic RBM28-mCherry was distributed throughout the nucleoplasm, where it partially colocalized with GFP-p53 (Fig. 5C). Meanwhile, the proximity labeling assay showed that the binding of p53 and RBM28 was increased in response to ADR in a dose-dependent manner (Fig. 5D). These findings revealed that RBM28 translocated from the nucleolus to the nucleoplasm, where it interacts with p53, upon DNA-damaging agent treatment.

The DNA damage response is a signal transduction pathway involved in many processes of kinase cascade activation (20), reflecting the possibility that RBM28 is regulated by some key molecules through posttranslational modification in the DNA damage pathway. Both an ATM inhibitor (AZD1390) and a Chk1 inhibitor (LY2606368) reduced nucleoplasmic localization of RBM28 in HCT116 cells upon ADR treatment (Fig. 5E). Likewise, siRNAs targeting both Chk1 and Chk2 also impeded nucleoplasmic localization of RBM28 in HCT116 cells upon ADR treatment (Fig. 5, F and G), as AZD1390 and LY2606368 could also suppress the activity of both Chk1 and Chk2 (21), indicating that Chk1/Chk2 promote the nucleolar–nucleoplasmic translocation of RBM28 induced by ADR.

### Chk1/Chk2 phosphorylates S122 of RBM28 to induce the nucleolar–nucleoplasmic translocation of RBM28 upon ADR treatment

Then, we analyzed the amino acid sequence of RBM28 and found three potential Chk1/Chk2 phosphorylation sites, namely, Thr86 (T86), Ser122 (S122), and Ser343 (S343), according to a phosphorylation prediction tool called the Grouped-based Prediction System (GPS5.0) (22). Phospho-defective mutants (S/T to A) and phospho-mimetic mutants (S/T to D) of these putative phosphorylation sites were generated. Interestingly, only the RBM28 S122A mutant was predominantly localized in the nucleolus, whereas other mutants were distributed throughout the nucleus (Fig. 6A), indicating that the phosphorylation status of RBM28 at S122 may be crucial to determine the subcellular localization of RBM28.

Indeed, using anti-phospho-S/T Chk1/Chk2 substrate antibody, the phosphorylation of WT RBM28 was enhanced when cotransfected with HA-Chk1 or HA-Chk2 (Fig. 6B), and only the S122A mutant diminished the Chk1/Chk2-induced phosphorylation of RBM28 (Fig. 6C), demonstrating that S122 is the key site for phosphorylation by Chk1/Chk2. Notably, S122 status did not affect the interaction of RBM28 with Chk1/Chk2 (Fig. S7). Furthermore, we generated a specific anti-phospho-Ser122 (p-S122) antibody and found that S122 phosphorylation of RBM28 was dramatically increased by either Chk1 or Chk2 in cells transiently cotransfected with their plasmids (Fig. 6D). More importantly, ADR treatment

was found to increase RBM28-S122 phosphorylation (Fig. 6E) using an anti-p-S122 antibody. Immunofluorescence assay showed that the nucleoplasmic localization of WT RBM28, but not the RBM28 S122A mutant, was increased upon cotransfection with either HA-Chk1 or HA-Chk2 (Fig. 6F), whereas the RBM28 S122A mutant prevented the nucleoplasmic localization of RBM28 induced by ADR (Fig. 6G). These results revealed that Chk1/Chk2 may phosphorylate S122 of RBM28 to induce nucleolar–nucleoplasmic translocation of RBM28 upon ADR treatment.

## Discussion

In this report, as illustrated in Figure 7, chemotherapeutic drugs (e.g., ADR) could activate Chk1/2 to phosphorylate S122 of RBM28, promoting the translocation of RBM28 from the nucleolus to the nucleoplasm, where RBM28 interacts with the DNA-binding domain of p53 to inhibit p53 transcriptional activity. Our findings provide mechanistic insights into how cancer cells convert stress signals into a cellular response linking the nucleolus to regulation of the tumor suppressor p53.

As a nucleolar component of spliceosomal small nuclear ribonucleoproteins (snRNPs), RBM28 is involved in snRNP maturation and comprises four RNA recognition motifs (RRMs 1–4) and an extremely acidic region of 32 amino acids between RRM2 and RRM3 (23). A homozygous loss-of-function mutation in RBM28 was reported to underlie alopecia, neurological defects, and endocrinopathy syndrome (1, 24). A deleterious mutation in the RRM3 domain of Nop4p, its yeast ortholog, was found to confer growth and pre-rRNA processing defects, suggesting a role for RBM28 in ribosome biogenesis (25). Here, we determined for the first time that RBM28 may act as an oncogene to promote growth of cancer cells, as RBM28 depletion significantly activates the p53 pathway and inhibits cancer cell survival and growth, and that high RBM28 expression predicts a poor prognosis in cancer patients. These findings indicate that RBM28 may be a potential biomarker and therapeutic target for cancers.

Links between the nucleolus and cellular stress were proposed based on the finding that the nucleolus participates in regulating the abundance of stress-responsive p53 (4). The notion that the nucleolus plays a role in regulating cellular stress represents at least two aspects of the same idea: p53 activation by nucleolar proteins. One hypothesis emphasizes mechanisms mainly involved in changes in the protein–protein interactions, in which the nucleolus is a sensor for cellular stress, with stress-induced nucleoplasmic translocation of nucleolar proteins, such as NPM1 and GLTSCR2, initiating p53 activation (6, 26). The other hypothesis focuses on a translation-mediated mechanism, where the engagement of ribosomal proteins (RPs), mainly RPL5, RPL11, and RPL23, is implicated in increased mRNA translation, with less emphasis on their translocation (27). In this report, upon

transfected with siRNAs targeting Chk1 and Chk2 for 48 h and treated with the indicated concentrations of ADR in the presence of MG132 (10  $\mu$ M, 6 h). The data are the mean  $\pm$  SD, n = 5; ns, no significance, \*\* $p$  < 0.01, \*\*\* $p$  < 0.001, \*\*\*\* $p$  < 0.0001 by unpaired Student's  $t$  test. Act D, actinomycin D; ADR, adriamycin; CPT, camptothecin.

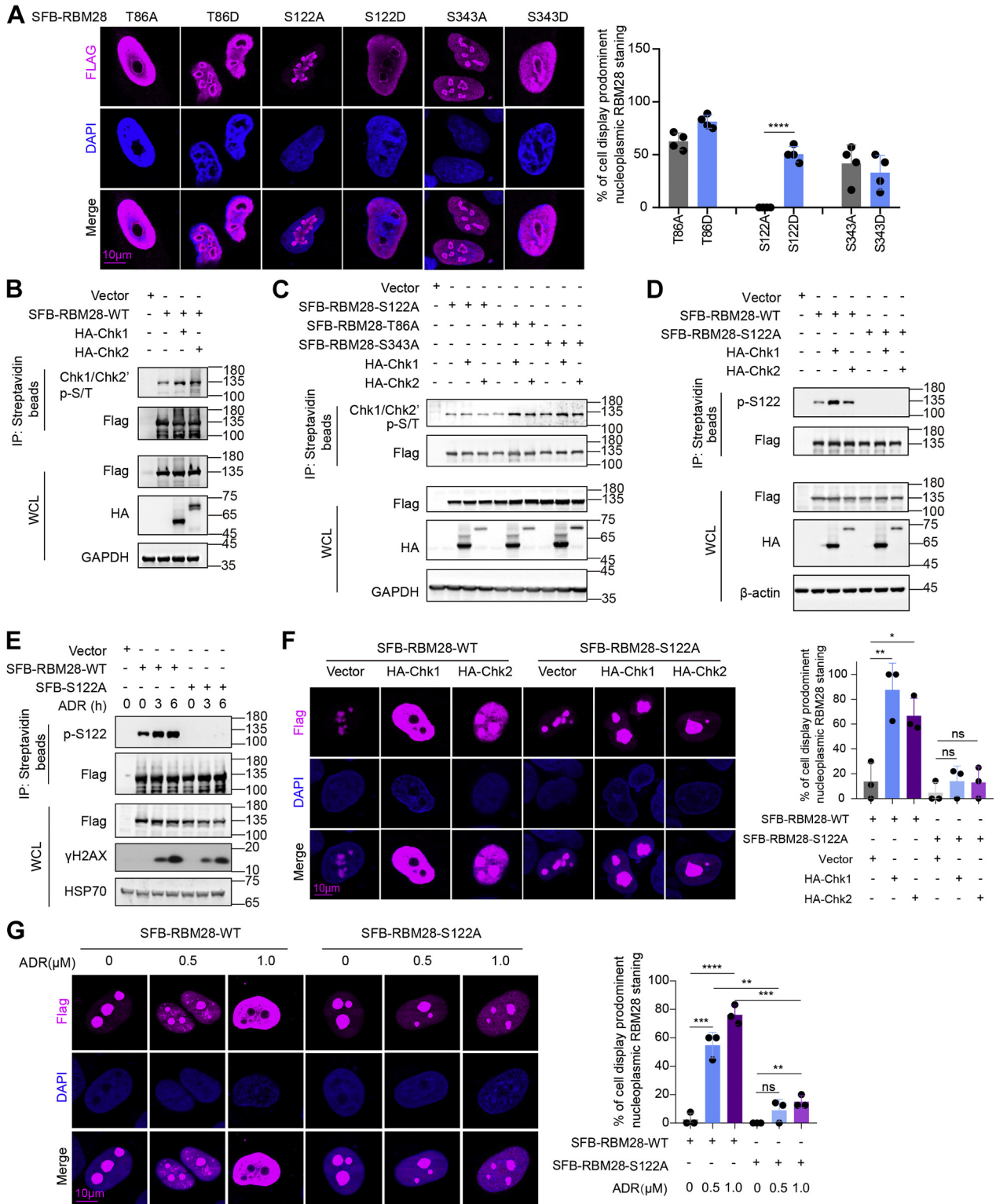


**Figure 6. Chk1/2 phosphorylates RBM28 at S122 upon ADR treatment.** *A*, immunofluorescence assays were performed to observe the subcellular localization of SFB-RBM28 (violet, anti-FLAG) and nuclei (blue) in U2OS cells transfected with the indicated RBM28 mutants for 48 h in the presence of MG132 (10  $\mu$ M, 6 h). The data are the mean  $\pm$  SD,  $n = 4$ . \*\*\*\* $p < 0.0001$  by unpaired Student's *t* test. *B–D*, HEK293T cells transfected with the indicated plasmids for 48 h in the presence of MG132 (10  $\mu$ M, 6 h) were immunoprecipitated with streptavidin beads, followed by Western blotting. *E*, HEK293T cells transfected with the indicated plasmids were treated with ADR (4  $\mu$ M) for the indicated times, followed by IP using streptavidin beads and Western blotting using an anti-phospho-Ser122 antibody. *F*, immunofluorescence assays were performed to observe the subcellular localization of RBM28(violet) and nuclei (blue) of HEK293T cells transfected with the indicated plasmids for 48 h in the presence of MG132 (10  $\mu$ M, 6 h). The data are the mean  $\pm$  SD,  $n = 3$ ; ns, no significance, \* $p < 0.05$ , \*\*\* $p < 0.001$  by unpaired Student's *t* test. *G*, immunofluorescence assays were performed to observe the subcellular localization of RBM28 (violet) and nuclei (blue) of SFB-RBM28-WT or SFB-RBM28-S122A in HEK293T cells in the presence of the indicated concentrations of ADR for 3 h. The scale bar represents 10  $\mu$ m. The data are the mean  $\pm$  SD,  $n = 3$ ; ns, no significance, \*\* $p < 0.01$ , \*\*\* $p < 0.001$ , \*\*\*\* $p < 0.0001$  by unpaired Student's *t* test. ADR, adriamycin; HEK, human embryonic kidney.

## RBM28 inhibits p53 via nucleolus–nucleoplasm translocation

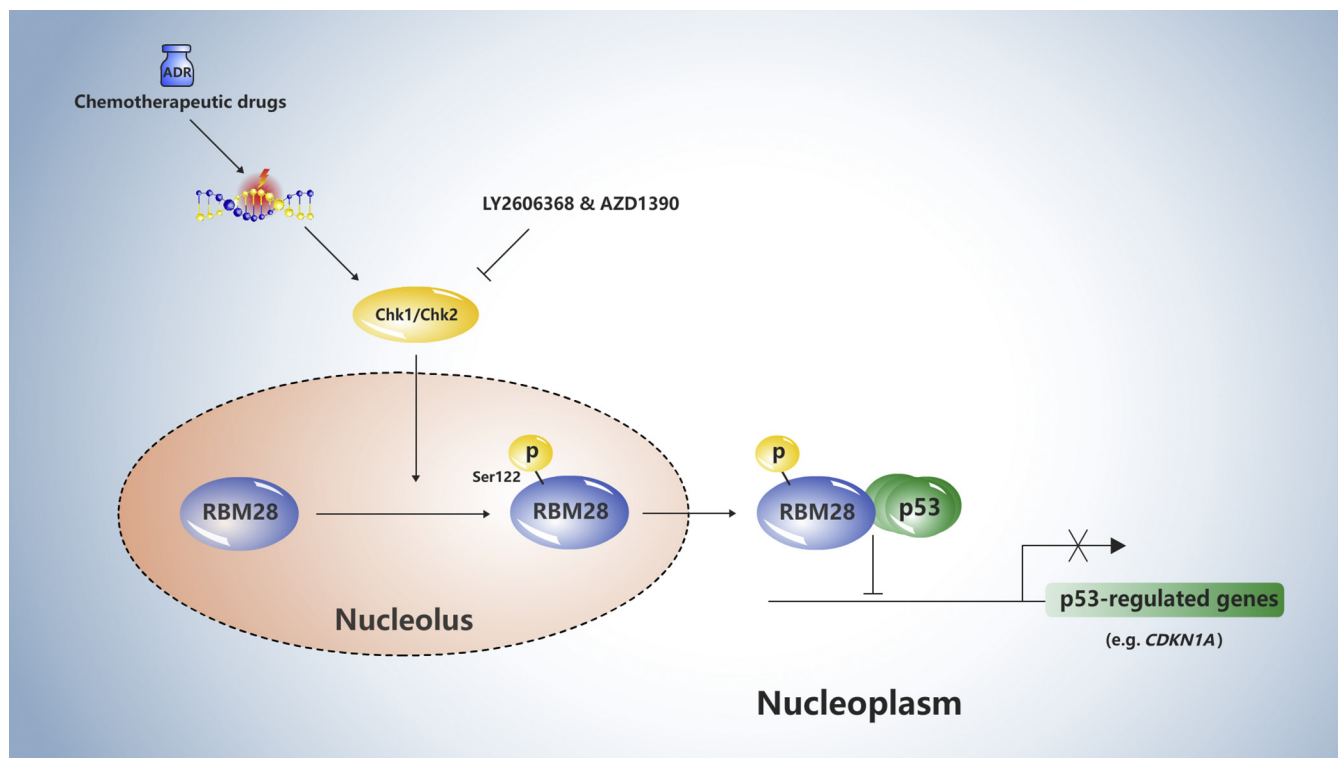


**Figure 7.** A proposed model shows how RBM28 regulates transcriptional activity of p53 in a phosphorylation-dependent manner. Chemotherapeutic drugs (e.g., ADR) can activate Chk1/2 to phosphorylate S122 of RBM28, promoting the translocation of RBM28 from the nucleolus to the nucleoplasm, where RBM28 interacts with the DNA-binding domain of p53 to inhibit p53 transcriptional activity. ADR, adriamycin.

nucleolar stress, such as the ADR treatment, we uncovered a novel repressive mechanism of RBM28 on p53 activity, where RBM28 is translocated to the nucleoplasm from the nucleolus, which is mediated by phosphorylation of RBM28 at S122 by Chk1/Chk2. These findings indicate that RBM28 may act as a nucleolar stress sensor in response to DNA damage stress.

p53, as the “guardian of the genome”, is an established tumor suppressor gene that activates the transcription of multiple target genes (28). The most common and well-characterized TP53 mutations are missense mutations in the DNA-binding domain, implying that this feature of p53 is crucial for tumor suppression (29). In this study, we found that nucleoplasmic translocation of RBM28 is essential for its binding to p53, which could be induced by chemotherapeutic drugs (e.g., ADR). This finding may provide a novel explanation for WT p53 cancer cells’ greater resistance to chemotherapy. Therefore, some compounds that disrupt the RBM28–p53 interaction may be used to increase the sensitivity of cancer cells with WT p53 to chemotherapy. Notably, Chk1 has been proposed as an attractive target in p53-deficient tumors but not WT p53 cancers, because p53 can partially compensate for the loss of Chk1-mediated cell cycle regulation (30, 31). Here, we found that a Chk1 inhibitor (LY2606368) could block the translocation of RBM28 from the nucleolus to the nucleoplasm, which in turn leads to lack the inhibition of RBM28 on p53. In this situation, cancer cells with higher RBM28 levels may be more sensitive to Chk1 inhibitors, suggesting that RBM28 may serve as a useful biomarker for

predicting Chk1/Chk2 inhibitors sensitivity in cancer patients with WT p53.

### Experimental procedures

#### Reagents

The following reagents were used for cells: MG132 (Selleck; S2619), AZD1390 (Selleck; S8680), LY2606368 (Selleck; S7178), ADR (Selleck, S1208), ActD (APEXbio, A4448), etoposide (Selleck; S1225), and camptothecin (Selleck; S1288).

#### Cell culture and treatments

The human embryonic kidney 293 cells (HEK293T), U2OS, HCT116, A375, and SaOS2 were obtained from ATCC, HCT116 p53<sup>-/-</sup> cells were from Dr Yuxin Yin (Peking University Health Science Center), and all the cells were maintained in Dulbecco’s modified Eagle’ medium (Life Technologies) supplemented with 10% fetal bovine serum (Life Technologies) with 5% CO<sub>2</sub> at 37 °C. All cell lines used in this study were authenticated using short-tandem repeat profiling less than 6 months prior when this project was initiated, and the cells were not cultured for more than 2 months. The cells were negative for *mycoplasma* and tested by PCR monthly.

#### Plasmids

HA-Chk1, HA-Chk2, Myc-p53, HA-p53, and related truncation constructs were cloned into a pCDNA3.1 vector. SFB-RBM28, the related truncation constructs, and S/T to A/D mutants were cloned into a pSIN vector through infusion.

Sequences targeting RBM28 were cloned into a lenti-CRISPR V2 plasmid (Addgene, 52961). The shRNA expression constructs were in the pLKO.1-puro backbone.

### Transfection experiments

Chk1 and Chk2 siRNAs were synthesized by RiboBio. Transfection was performed according to the manufacturer's instructions using Lipofectamine RNAiMAX transfection reagent (Invitrogen) and 50 nM siRNA. Transient transfection of HEK293T cells was performed with PEI (25 kDa), and the cells were collected after 48 h for subsequent assay and lentiviral packaging. The siRNAs used for RT–PCR are listed in [Table S1](#).

### Colony formation assay

Stable HCT116 and U2OS cells were seeded at a density of 500 per well in 6-well plates. After 2 weeks, the cell clones were fixed in methanol and stained with 0.1% crystal violet. Cell clones containing more than 50 cells were counted.

### Immunohistochemistry

Immunohistochemistry staining was performed using 3  $\mu$ m sections. The primary antibodies against Ki-67 were diluted 1:400 and then incubated at 4 °C overnight in a humidified container. After three washes with PBS, the tissue slides were treated with a nonbiotin horseradish peroxidase detection system according to the manufacturer's instructions (Dako).

### Western blot and immunoprecipitation

For Western blot analysis, the cells were lysed in RIPA buffer (50 mM Tris–HCl, 150 mM NaCl, 5 mM EDTA, and 0.5% NP-40) containing protease inhibitor and phosphatase inhibitor cocktails (Thermo Scientific). The lysates were cleared by centrifugation at 12,000 rpm for 20 min at 4 °C. The cleared lysates were incubated with antibody beads or agarose overnight at 4 °C or with antibodies at 4 °C for 2 h followed by incubation with protein A/G PLUS-Agarose (Santa Cruz) at 4 °C for 2 h. Precipitates were then washed five times with cold RIPA buffer and eluted with 5 $\times$  SDS sample buffer. The immunoprecipitates were separated by SDS–PAGE and transferred to a PVDF membrane (Millipore). The membranes were blocked in TBS containing 5% nonfat milk and 0.1% Tween-20, probed with primary antibodies overnight at 4 °C, washed five times with TBS containing 5% nonfat milk and 0.1% Tween-20, and then incubated with horseradish peroxidase-conjugated secondary antibodies (Promega). Clarity Western ECL substrate (Bio–Rad) was used for detection.

### MTT assay

Stable HCT116 and U2OS cells were seeded in 96-well microplates at a density of 2000 cells per well, and 3-(4, 5-dimethylthiazol-2-yl)-2, 5-diphenyltetrazolium bromide assay was used to assess cell viability per day for five continuous days.

### Immunofluorescence

Cells were seeded into confocal dishes (NEST Biotechnology) and fixed with 4% paraformaldehyde for 10 min at room temperature. After permeabilization with 0.5% Triton X-100 for 10 min, the cells were blocked with 5% goat serum and incubated with primary antibody overnight at 4 °C. The next day, the cells were washed and incubated with secondary antibody at room temperature for 1 h, and then the nuclei were labeled by using Hoechst 33342 for 5 min.

### Luciferase reporter assay

Briefly, HCT116 and U2OS cells were plated in 24-well plates and then transiently transfected with 250 ng *CDKN1A* promoter containing *Firefly* luciferase reporter plasmid (Promega E1330). To normalize the transfection efficiency, the cells were also cotransfected with 8 ng of pRL-TK (*Renilla* luciferase). Luciferase activity was measured in at least three independent experiments using a Dual-Luciferase Assay kit (Promega) after transfection for 48 h.

### Chromatin immunoprecipitation

This procedure was performed, as described by the ChIP kit (Millipore, 17–10085 & 17–1008). Briefly, 15-cm plates were seeded with cells of each of the tested cell lines and allowed to grow to 70% to 80% confluence. To fix cells, complete cell fixative solution (1/10th the volume of the growth medium volume) was added to the existing culture medium. The fixation reaction was stopped by adding stop solution (1/20th the volume of the growth medium volume) to the existing culture medium. The cells were collected by centrifugation, and the nuclear pellet was resuspended in ChIP buffer. The cell lysate was subjected to sonication and then incubated with 3  $\mu$ g of antibodies overnight, followed by incubation with protein A/G agarose overnight at 4 °C. Bound DNA–protein complexes were eluted, and cross-links were reversed after a series of washes. The purified DNA was resuspended in TE buffer for PCR. The primers for the indicated promoters are shown in [Table S1](#).

### Real-time quantitative PCR analysis

Total RNA was extracted from the samples (RNAprep pure cell/bacteria kit; TIANGEN), quantified by using a Nanodrop 2000 spectrophotometer, and stored at –80 °C. One microgram of RNA was reverse transcribed using a HiScript II first Strand cDNA synthesis kit (Vazyme) following the manufacturer's recommendations. The transcripts were quantified by real-time qPCR using a Light-Cycler 480 instrument (Roche Diagnostics) and ChamQ SYBR qPCR Master Mix (Vazyme) according to the manufacturer's instructions.

### Xenograft tumor model

Animal studies were approved by the Animal Research Committee of Sun Yat-sen University Cancer Center. Male athymic BALB/C nude mice (4 weeks old) were obtained from

## RBM28 inhibits p53 via nucleolus–nucleoplasm translocation

NBRI of Nanjing University. Briefly,  $4 \times 10^6$  HCT116 cells were resuspended in 0.1 ml of PBS and subcutaneously injected into the flanks of the mice. Tumor volumes were measured twice a week and were calculated using the formula  $V = 0.5 \times \text{length} \times \text{width}^2$ . All mice were sacrificed 19 days after injection, and the xenograft tumors were isolated, photographed, and weighed.

### mRNA stability assay

To determine the *CDKN1A* mRNA half-life, RBM28-KO U2OS cells were incubated with ActD (5  $\mu\text{g/ml}$ ) and then collected at the indicated times. Total RNA was extracted by an RNAprep pure cell/bacteria kit (TIANGEN) and analyzed by RT-PCR.

### Statistical analysis

All statistical experiments were performed independently and in triplicate. Statistical analysis was carried out using GraphPad Prism software (version 8.0 for Windows). Two-tailed unpaired Student's *t* test was performed between two groups. The survival rates were calculated using the Kaplan–Meier method and analyzed by the log-rank test. Tumor growth for different groups was analyzed by two-way ANOVA. The data are the mean  $\pm$  SD. A *p* value  $<0.05$  indicated a significant difference.

### Antibodies

Anti-Flag (Cell Signaling Technology, 14793, 1:2000); anti-HA (Cell Signaling Technology, 3724, 1:2000); anti-Chk2 (Cell Signaling Technology, 3440, 1:1000); anti-p53 (Cell Signaling Technology, 2527, 1:1000); anti-acetyl-K382 p53 (Cell Signaling Technology, 2525, 1:1000); anti-phosphor-S15 p53 (Cell Signaling Technology, 9284, 1:1000); anti-IgG (Cell Signaling Technology, 2729, Immunoprecipitation/ChIP); anti-Ki-67 (Cell Signaling Technology, 12202S, 1:400); anti-GAPDH (Proteintech, 10494-1-AP, 1:1000); anti-RBM28 (Proteintech, 16484-1-AP, 1:1000); anti-p21 (Proteintech, 60214-1-Ig, 1:1000); anti-HSP70 (Santa Cruz, sc-24, 1:5000); and anti-p53 (Santa Cruz, sc-126, 1:1000) (Table S2).

### Data availability

Raw data of the RNA-seq was uploaded to Genome Sequence Archive for Human (GSA for Human; <https://ngdc.cncb.ac.cn/gsa-human/>) with the accession code HRA001416. Other data sets used for the present study are available from the corresponding author upon reasonable request.

**Supporting information**—This article contains supporting information.

**Acknowledgments**—This work was supported by grants from the National Key Research and Development Program of China (2016YFA0500304), NSFC grants (81772922, 82002917, 82030090), Science and Technology Program of Guangzhou (202002020092), and Postdoctoral Funding (2020M683037).

**Author contributions**—X. L., Liwen Zhou, Li Zhong, and Y. W. conceptualization; X. L. validation; X. L., Liwen Zhou, and Y. W. formal analysis; X. L., Liwen Zhou, J. Z., Li Zhong, and Y. W. investigation; X. L. writing—original draft; X. L. and Y. W. visualization; X. L., Liwen Zhou, R. Z., T. K., and Y. W. project administration; T. K. and Y. W. supervision; T. K. writing—review and editing.

**Conflict of interest**—The authors declare that they have no conflicts of interest with the contents of this article.

**Abbreviations**—The abbreviations used are: ActD, actinomycin D; ADR, adriamycin; ChIP, chromatin immunoprecipitation; PTMs, posttranslational modifications; RBP, RNA-binding protein; RPs, ribosomal proteins; RRM, RNA recognition motif; snRNPs, small nuclear ribonucleoproteins.

### References

1. Nousbeck, J., Spiegel, R., Ishida-Yamamoto, A., Indelman, M., Shani-Adir, A., Adir, N., Lipkin, E., Bercovici, S., Geiger, D., van Steensel, M. A., Steijlen, P. M., Bergman, R., Bindereif, A., Choder, M., Shalev, S., *et al.* (2008) Alopecia, neurological defects, and endocrinopathy syndrome caused by decreased expression of RBM28, a nucleolar protein associated with ribosome biogenesis. *Am. J. Hum. Genet.* **82**, 1114–1121
2. Orsolich, I., Jurada, D., Pullen, N., Oren, M., Eliopoulos, A. G., and Volarevic, S. (2016) The relationship between the nucleolus and cancer: Current evidence and emerging paradigms. *Semin. Cancer Biol.* **37–38**, 36–50
3. Liu, Y., Deisenroth, C., and Zhang, Y. (2016) RP–MDM2–p53 pathway: Linking ribosomal biogenesis and tumor surveillance. *Trends Cancer* **2**, 191–204
4. Yang, K., Yang, J., and Yi, J. (2018) Nucleolar stress: Hallmarks, sensing mechanism and diseases. *Cell Stress* **2**, 125–140
5. Kodiha, M., Banski, P., and Stochaj, U. (2011) Computer-based fluorescence quantification: A novel approach to study nucleolar biology. *BMC Cell Biol.* **12**, 25
6. Yang, K., Wang, M., Zhao, Y. Z., Sun, X. X., Yang, Y., Li, X., Zhou, A. W., Chu, H. L., Zhou, H., Xu, J. R., Wu, M., Yang, J., and Yi, J. (2016) A redox mechanism underlying nucleolar stress sensing by nucleophosmin. *Nat. Commun.* **7**, 13599
7. Qin, H., Ni, H. W., Liu, Y. C., Yuan, Y. Q., Xi, T., Li, X. M., and Zheng, L. F. (2020) RNA-binding proteins in tumor progression. *J. Hematol. Oncol.* **13**, 90
8. Xiao, R., Chen, J.-Y., Liang, Z., Luo, D., Chen, G., Lu, Z. J., Chen, Y., Zhou, B., Li, H., Du, X., Yang, Y., San, M., Wei, X., Liu, W., Lécuyer, E., *et al.* (2019) Pervasive chromatin-RNA binding protein interactions enable RNA-based regulation of transcription. *Cell* **178**, 107–121.e18
9. Pereira, B., Billaud, M., and Almeida, R. (2017) RNA-binding proteins in cancer: Old players and new actors. *Trends Cancer* **3**, 506–528
10. Sutherland, L. C., Rintala-Maki, N. D., White, R. D., and Morin, C. D. (2005) RNA binding motif (RBM) proteins: A novel family of apoptosis modulators? *J. Cell. Biochem.* **94**, 5–24
11. Sun, X. N., Jia, M. Q., Sun, W., Feng, L., Gu, C. D., and Wu, T. H. (2019) Functional role of RBM10 in lung adenocarcinoma proliferation. *Int. J. Oncol.* **54**, 467–478
12. Yuan, M., Eberhart, C. G., and Kai, M. (2014) RNA binding protein RBM14 promotes radio-resistance in glioblastoma by regulating DNA repair and cell differentiation. *Oncotarget* **5**, 2820–2826
13. Sebestyen, E., Singh, B., Minana, B., Pages, A., Mateo, F., Pujana, M. A., Valcarcel, J., and Eyras, E. (2016) Large-scale analysis of genome and transcriptome alterations in multiple tumors unveils novel cancer-relevant splicing networks. *Genome Res.* **26**, 732–744

14. Best, M. G., Sol, N., In 't Veld, S. G. J. G., Vancura, A., Muller, M., Niemeijer, A. L. N., Fejes, A. V., Fat, L. A. T. K., In 't Veld, A. E. H., Leurs, C., Le Large, T. Y., Meijer, L. L., Kooi, I. E., Rustenburg, F., Schellen, P., *et al.* (2017) Swarm intelligence-enhanced detection of non-small-cell lung cancer using tumor-educated platelets. *Cancer Cell* **32**, 238–252
15. Zhao, Y., Lu, S. L., Wu, L. P., Chai, G. L., Wang, H. Y., Chen, Y. Q., Sun, J., Yu, Y., Zhou, W., Zheng, Q. H., Wu, M., Otterson, G. A., and Zhu, W. G. (2006) Acetylation of p53 at lysine 373/382 by the histone deacetylase inhibitor depsipeptide induces expression of p21(Waf1/Cip1). *Mol. Cell Biol.* **26**, 2782–2790
16. Sabapathy, K., and Lane, D. P. (2019) Understanding p53 functions through p53 antibodies. *J. Mol. Cell Biol.* **11**, 317–329
17. Boulon, S., Westman, B. J., Hutten, S., Boisvert, F.-M., and Lamond, A. I. (2010) The nucleolus under stress. *Mol. Cell* **40**, 216–227
18. Cheung-Ong, K., Giaever, G., and Nislow, C. (2013) DNA-damaging agents in cancer chemotherapy: Serendipity and chemical biology. *Chem. Biol.* **20**, 648–659
19. Rao, B., Lain, S., and Thompson, A. M. (2013) p53-based cyclotherapy: Exploiting the 'guardian of the genome' to protect normal cells from cytotoxic therapy. *Br. J. Cancer* **109**, 2954–2958
20. Ciccio, A., and Elledge, S. J. (2010) The DNA damage response: Making it safe to play with knives. *Mol. Cell* **40**, 179–204
21. Jin, M. H., and Oha, D. Y. (2019) ATM in DNA repair in cancer. *Pharmacol. Ther.* **203**, 107391
22. Wang, C. W., Xu, H. D., Lin, S. F., Deng, W. K., Zhou, J. Q., Zhang, Y., Shi, Y., Peng, D., and Xue, Y. (2020) GPS 5.0: An update on the prediction of kinase-specific phosphorylation sites in proteins. *Genomics Proteomics Bioinformatics* **18**, 72–80
23. Damianov, A., Kann, M., Lane, W. S., and Bindereif, A. (2006) Human RBM28 protein is a specific nucleolar component of the spliceosomal snRNPs. *Biol. Chem.* **387**, 1455–1460
24. Spiegel, R., Shalev, S. A., Adawi, A., Sprecher, E., and Tenenbaum-Rakover, Y. (2010) ANE syndrome caused by mutated RBM28 gene: A novel etiology of combined pituitary hormone deficiency. *Eur. J. Endocrinol.* **162**, 1021–1025
25. McCann, K. L., Teramoto, T., Zhang, J., Tanaka Hall, T. M., and Baserga, S. J. (2016) The molecular basis for ANE syndrome revealed by the large ribosomal subunit processome interactome. *Elife* **5**, e16381
26. Lee, S., Kim, J. Y., Kim, Y. J., Seok, K. O., Kim, J. H., Chang, Y. J., Kang, H. Y., and Park, J. H. (2012) Nucleolar protein GLTSCR2 stabilizes p53 in response to ribosomal stresses. *Cell Death Differ.* **19**, 1613–1622
27. Golomb, L., Volarevic, S., and Oren, M. (2014) p53 and ribosome biogenesis stress: The essentials. *FEBS Lett.* **588**, 2571–2579
28. Lane, D. P. (1992) p53, guardian of the genome. *Nature* **358**, 15–16
29. Giacomelli, A. O., Yang, X. P., Lintner, R. E., McFarland, J. M., Duby, M., Kim, J., Howard, T. P., Takeda, D. Y., Ly, S. H., Kim, E., Gannon, H. S., Hurhula, B., Sharpe, T., Goodale, A., Fritchman, B., *et al.* (2018) Mutational processes shape the landscape of TP53 mutations in human cancer. *Nat. Genet.* **50**, 1381–1387
30. Ferrao, P. T., Bukczynska, E. P., Johnstone, R. W., and McArthur, G. A. (2012) Efficacy of CHK inhibitors as single agents in MYC-driven lymphoma cells. *Oncogene* **31**, 1661–1672
31. Chen, Z. H., Xiao, Z., Gul, W. Z., Xue, J., Bui, M. H., Kovar, P., Li, G. Q., Wang, G., Tao, Z. F., Tong, Y. S., Lin, N. H., Sham, H. L., Wang, J. Y. J., Sowin, T. J., Rosenberg, S. H., *et al.* (2006) Selective Chk1 inhibitors differentially sensitize p53-deficient cancer cells to cancer therapeutics. *Int. J. Cancer* **119**, 2784–2794